Electronic Supplementary Material (ESI) for Dalton Transactions.
This journal is © The Royal Society of Chemistry 2019

Protonation and Electrochemical Properties of Bisphosphide Diiron Hexacarbonyl Complex Bearing Amino Groups on the Bridge

Takehiko Shimamura,[a] Yuki Maeno,[a] Kazuyuki Kubo,[a] Shoko Kume,[a] Claudio Greco,[b] and Tsutomu Mizuta [a] *

a Department of Chemistry, Graduate School of Science, Hiroshima University, Kagamiyama 1-3-1, Higashi-hiroshima 739-8526, Japan.

b Department of Earth and Environmental Science, University of Milano-Bicocca, Piazza della Scienza 1, 20126, Milan, Italy.

Table of Contents

14. Fig. S14. A $^{13}C\{^{1}H\}$ NMR spectrum of (μ-**5**')$[Fe(CO)_3]_2$ **3**.

15. Fig. S15. A $^{31}P\{^{1}H\}$ NMR spectrum of (μ-**5**')$[Fe(CO)_3]_2$ **3**.

16. Fig. S16. Plots of TsOH concentration vs increment of the current.

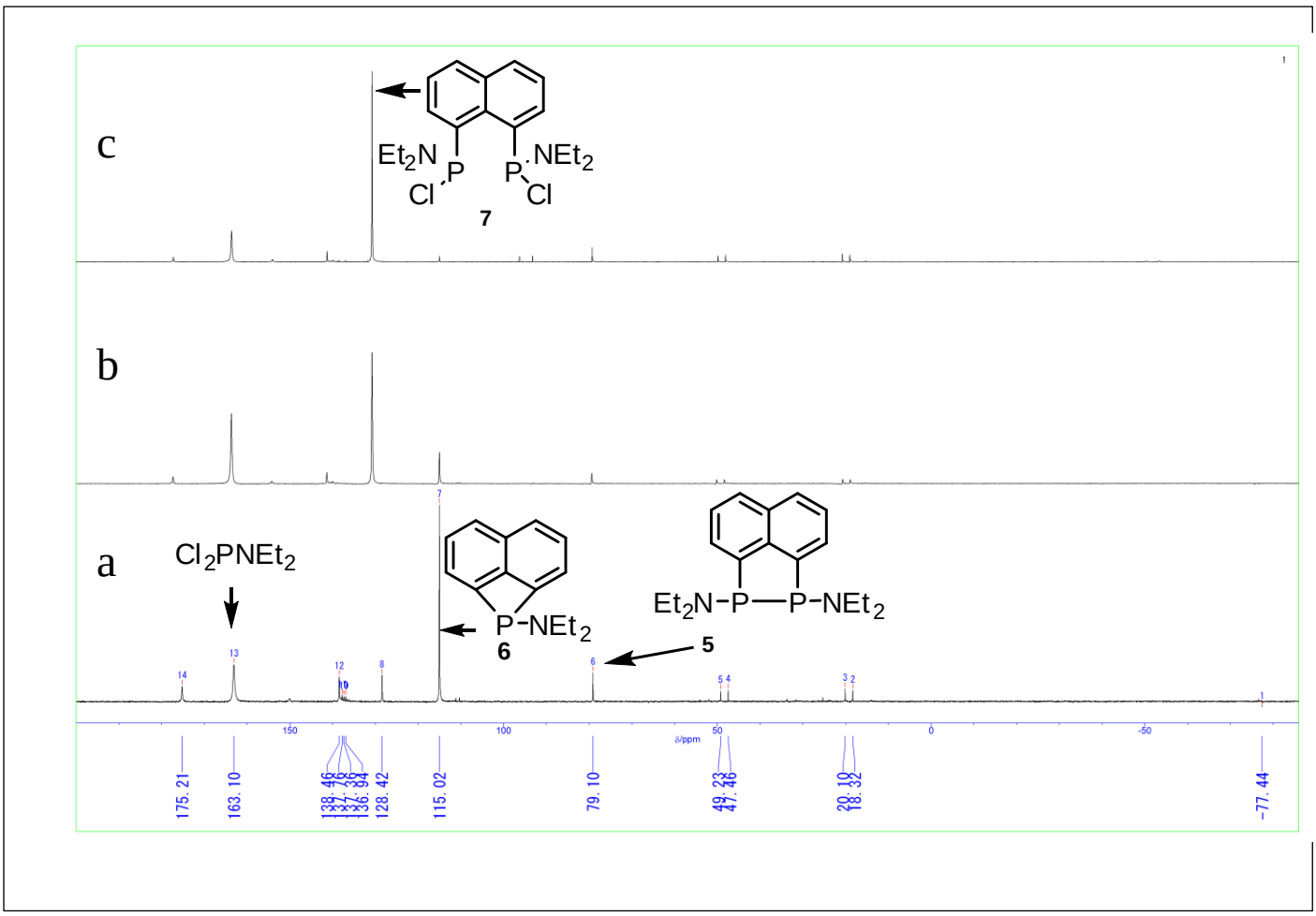

Fig. S1. $^{31}P\{^{1}H\}$ NMR spectra of the reaction mixture recorded after (a) 1h, (b) 12h, (c) 24h.

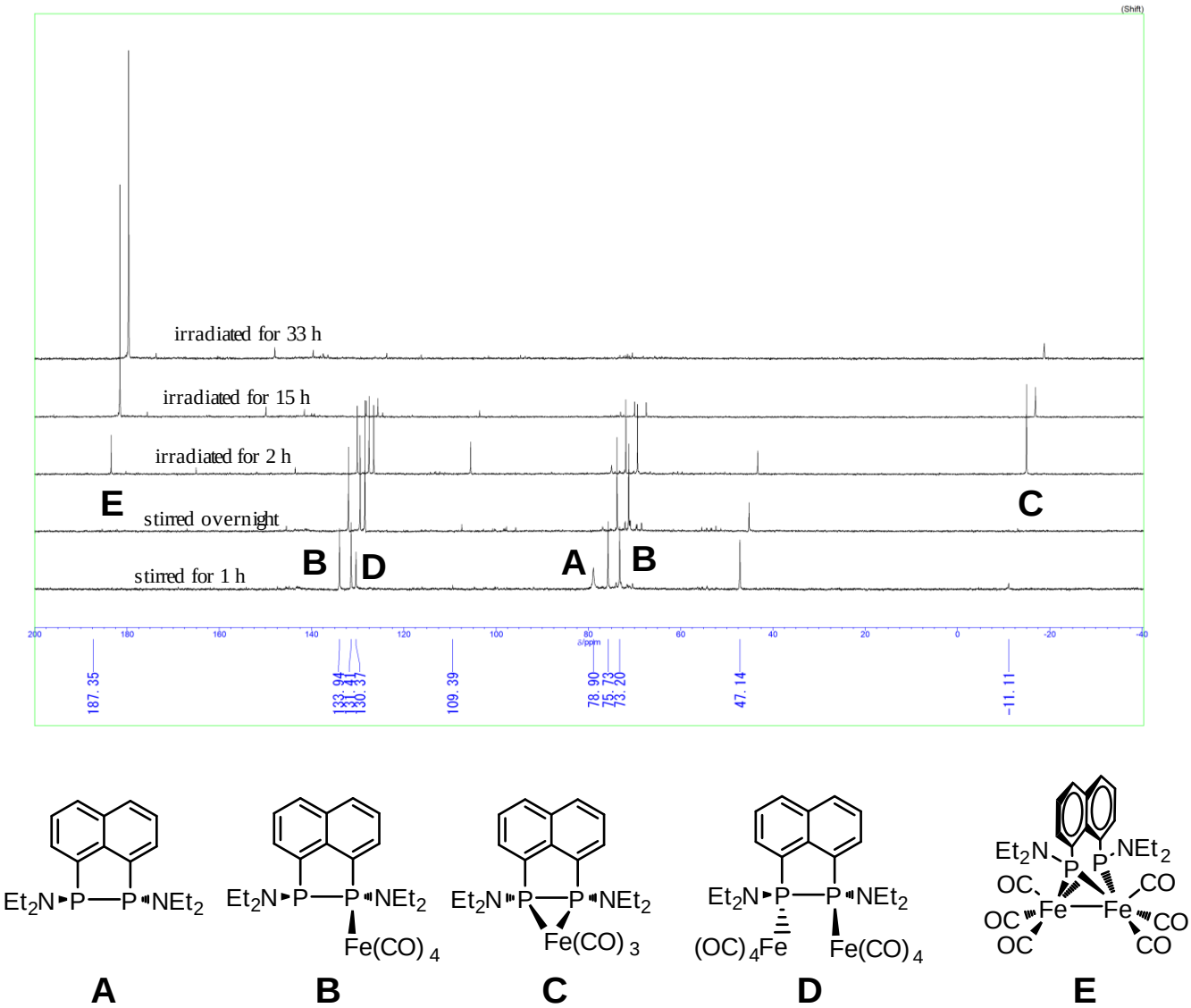

Fig. S2. $^{31}P\{^{1}H\}$ NMR spectra of the reaction mixture between ligand **A** and $Fe_2(CO)_9$.

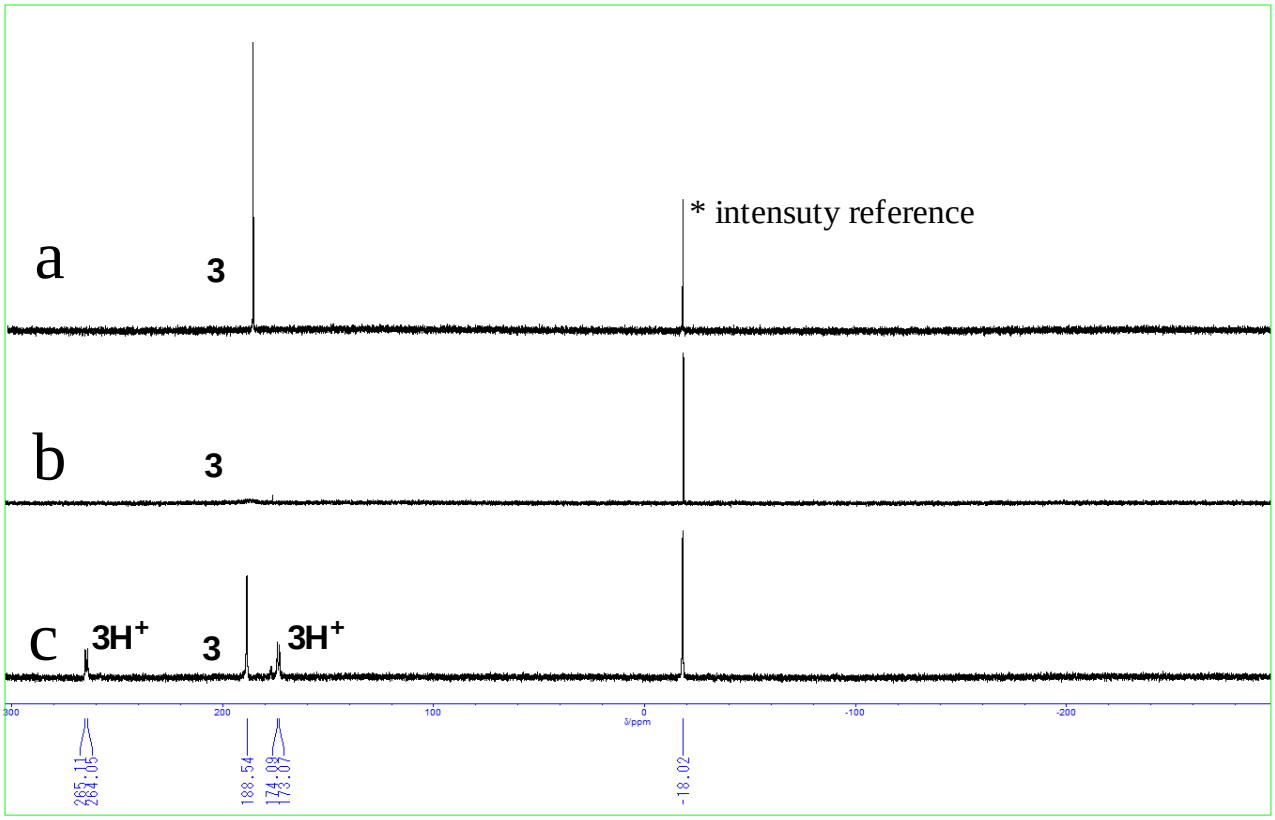

Figure S3. $^{31}P\{^{1}H\}$ NMR spectra of **3** (a), after addition of 3 eq of TsOH (b), and the same sample recorded at −55 ºC (c).

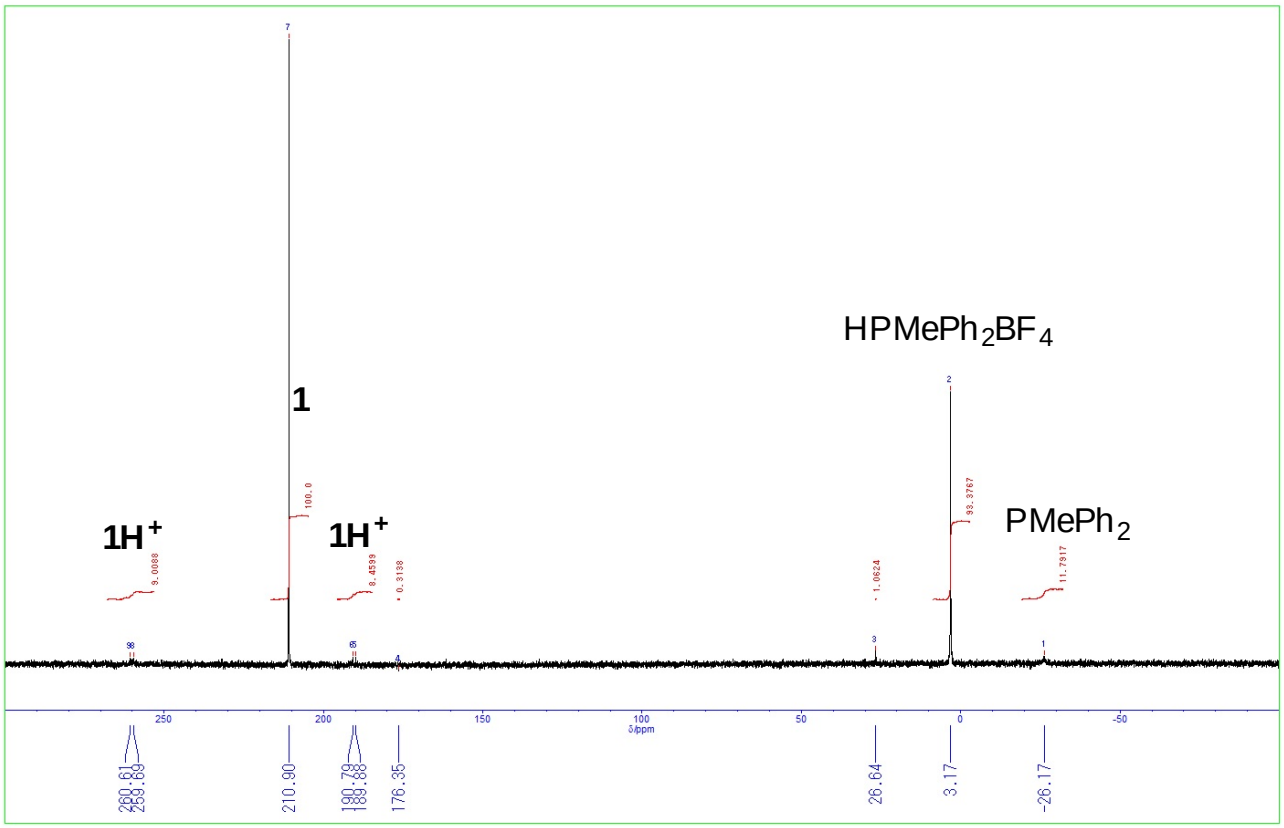

Fig. S4. ^{31}P NMR spectrum (NNE mode) of an equilibrium mixture between an [H-**1**]$^{+}$/**1** couple and an HPMePh$_2^{+}$/ PMePh$_2$,couple

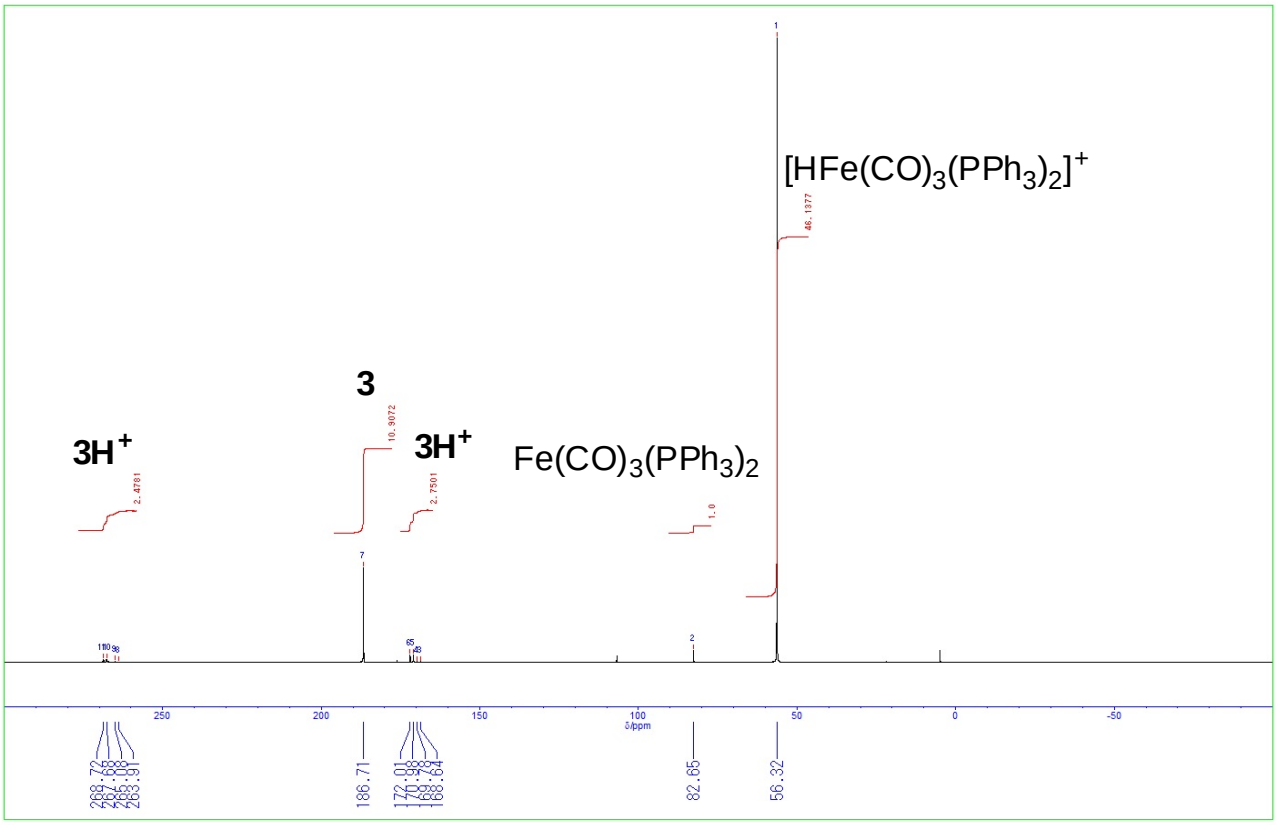

Fig. S5. ^{31}P NMR spectrum (NNE mode) of an equilibrium mixture between an **3**H$^+$/**3** couple and an $[HFe(CO)_3(PPh_3)_2]^+$/ $Fe(CO)_3(PPh_3)_2$ couple.

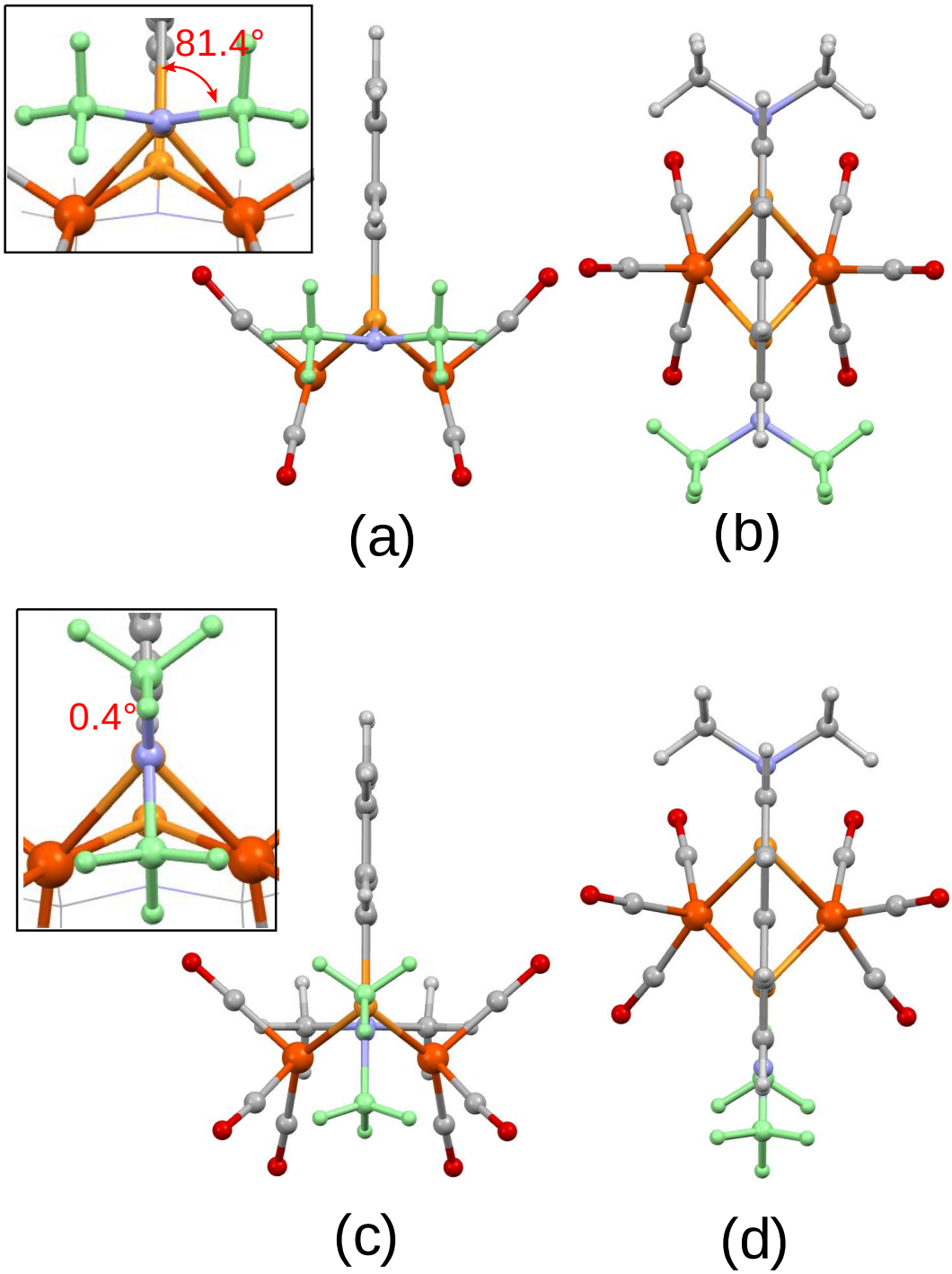

Fig. S6. Molecular structures of 3' obtained by DFT calculation. (a): a side view of energy minimum structure and torsion angle (inset), (b) a top view. (c): a side view of energy maximum structure and torsion angle (inset), (d) a top view.

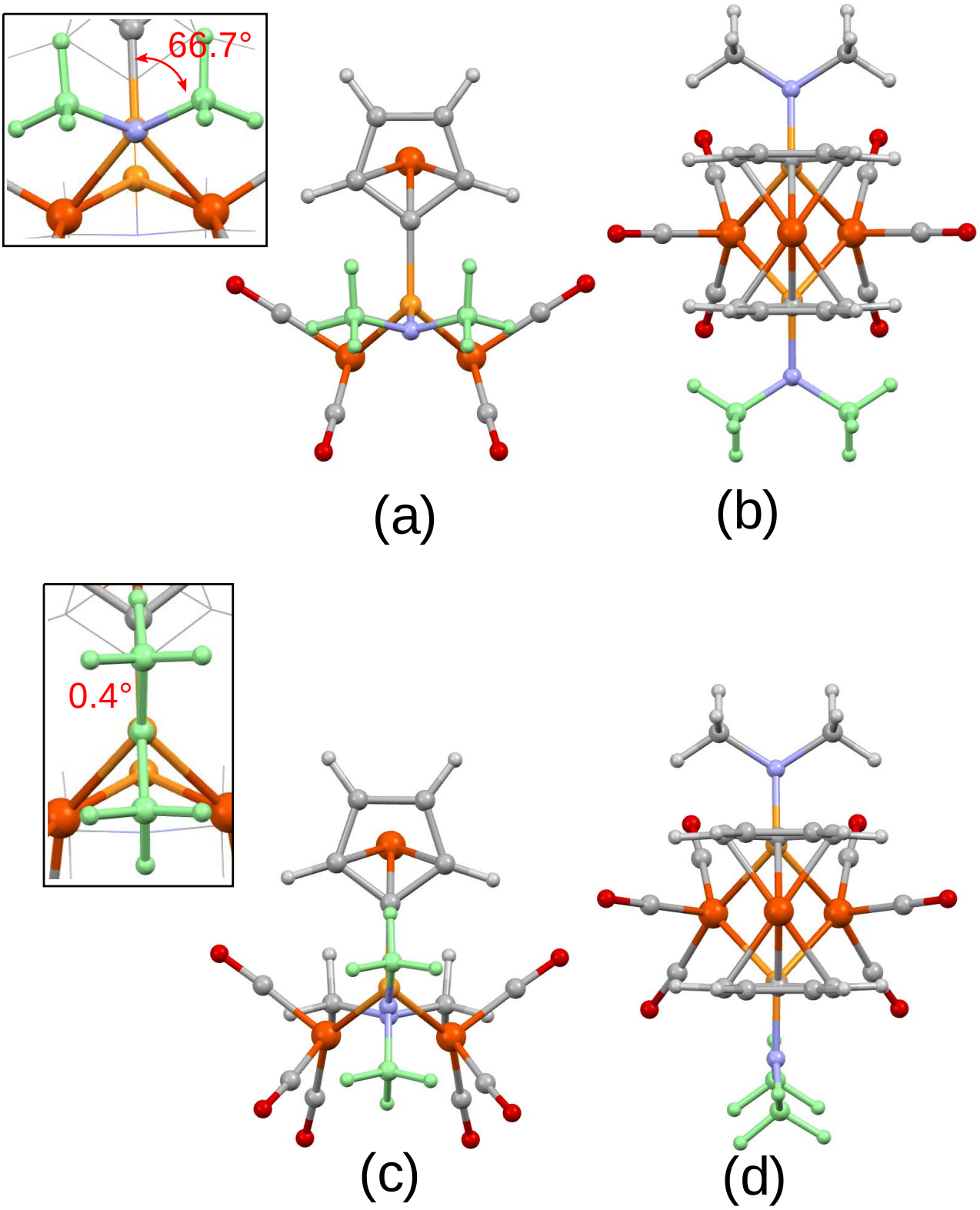

Fig. S7. Molecular structures of 1' obtained by DFT calculation. (a): a side view of energy minimum structure and torsion angle (inset), (b) a top view. (c): a side view of energy maximum structure and torsion angle (inset), (d) a top view.

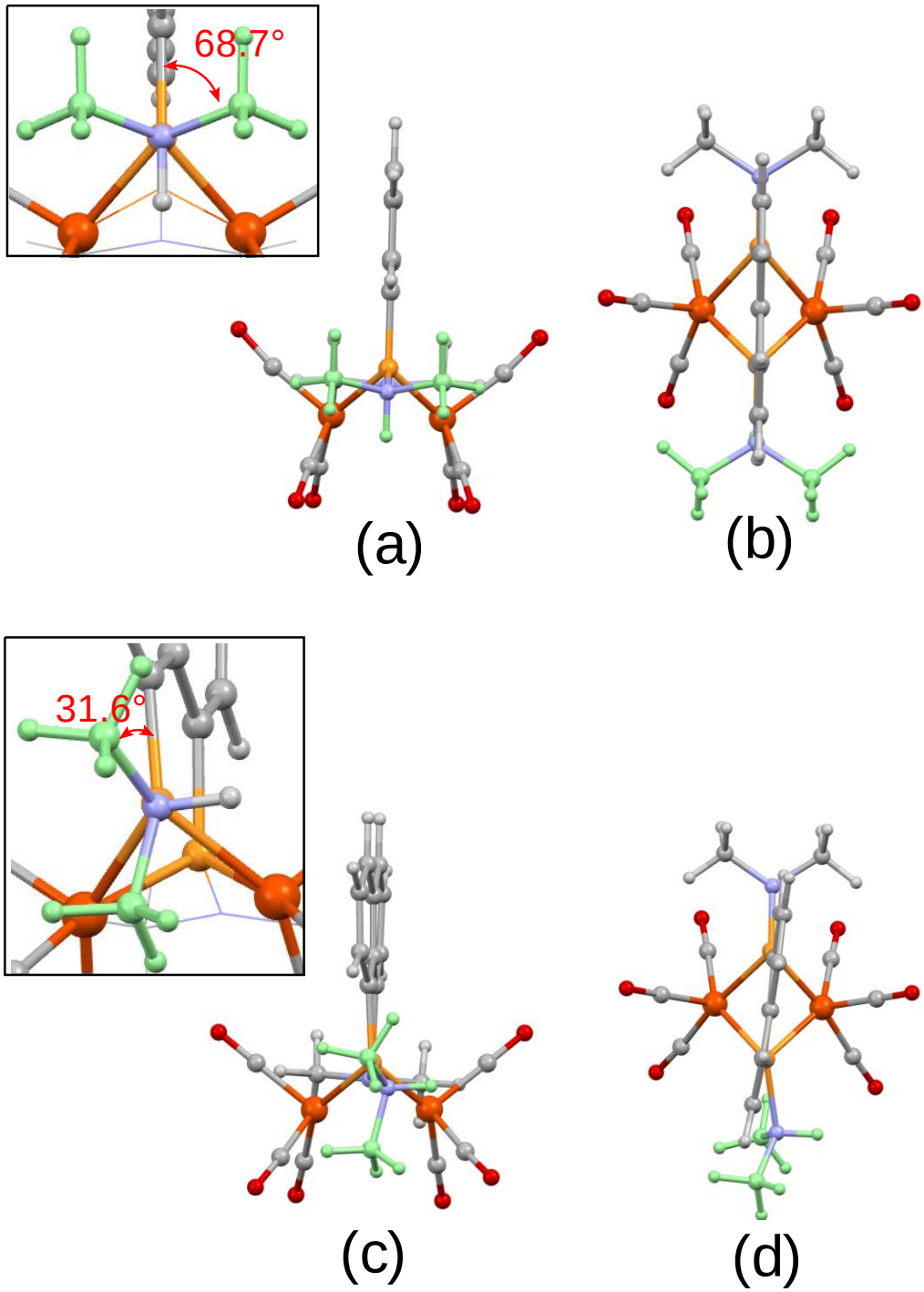

Fig. S8. Molecular structures of [H-**3**']$^{+}$ obtained by DFT calculation. (a): a side view of energy minimum structure and torsion angle (inset), (b) a top view. (c): a side view of energy maximum structure and torsion angle (inset), (d) a top view.

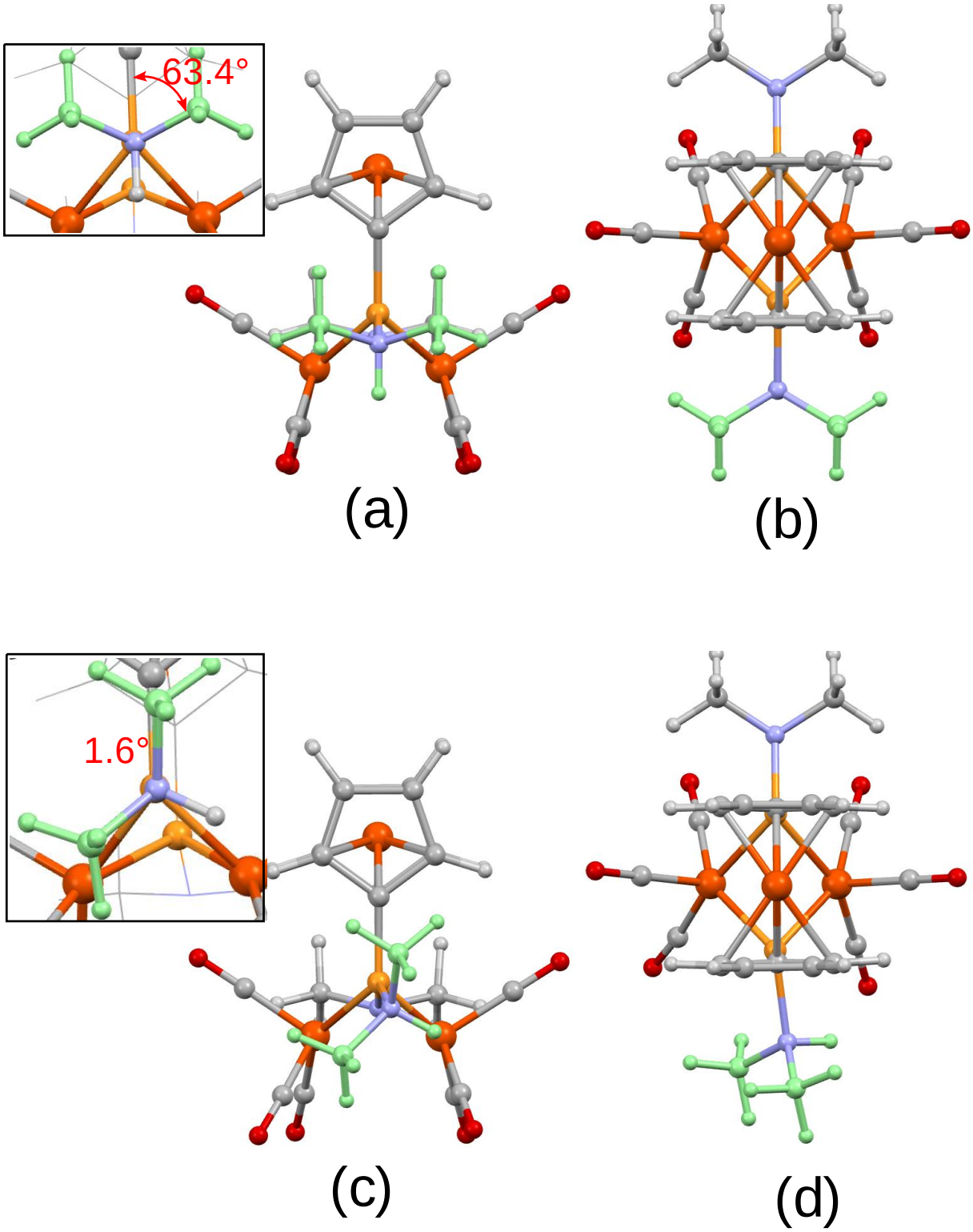

Figure S9. Molecular structures of [H-**1'**]$^+$ obtained by DFT calculation. (a): a side view of energy minimum structure and torsion angle (inset), (b) a top view. (c): a side view of energy maximum structure and torsion angle (inset), (d) a top view.

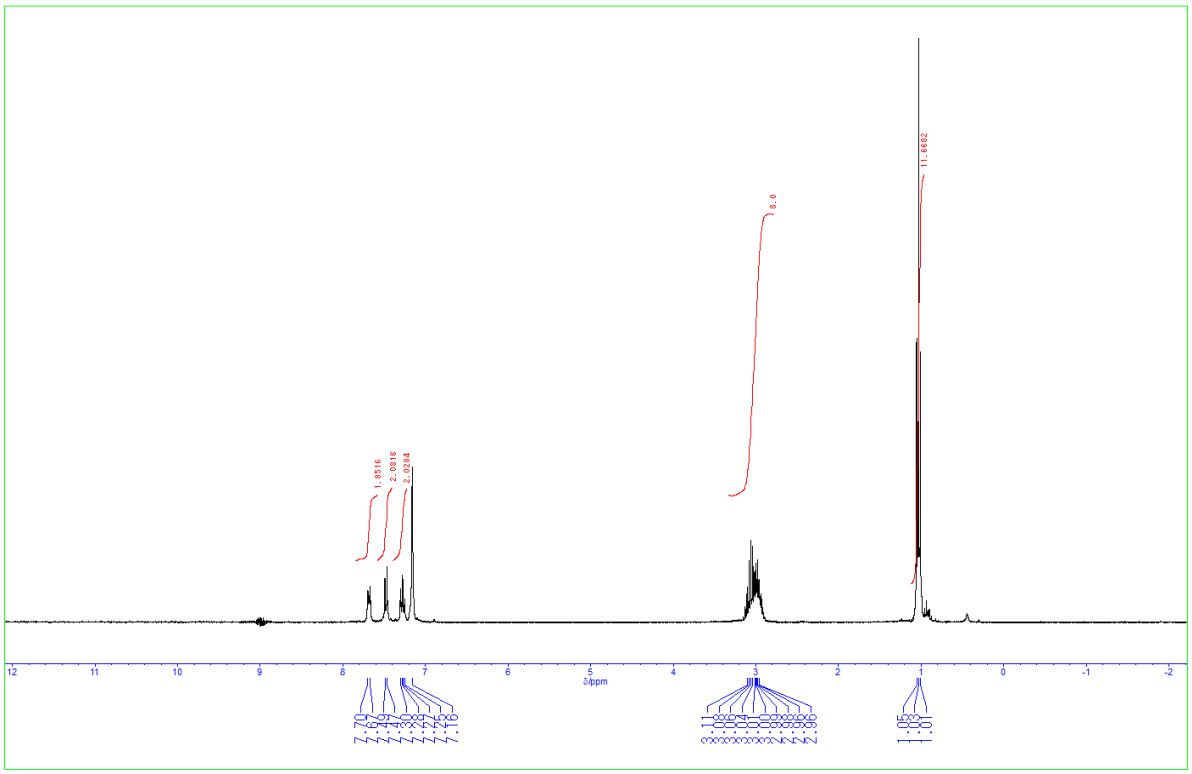

Fig. S10. A ^{1}H NMR spectrum of naphthylene-1,8-$Et_2NP–PNEt_2$ **5**

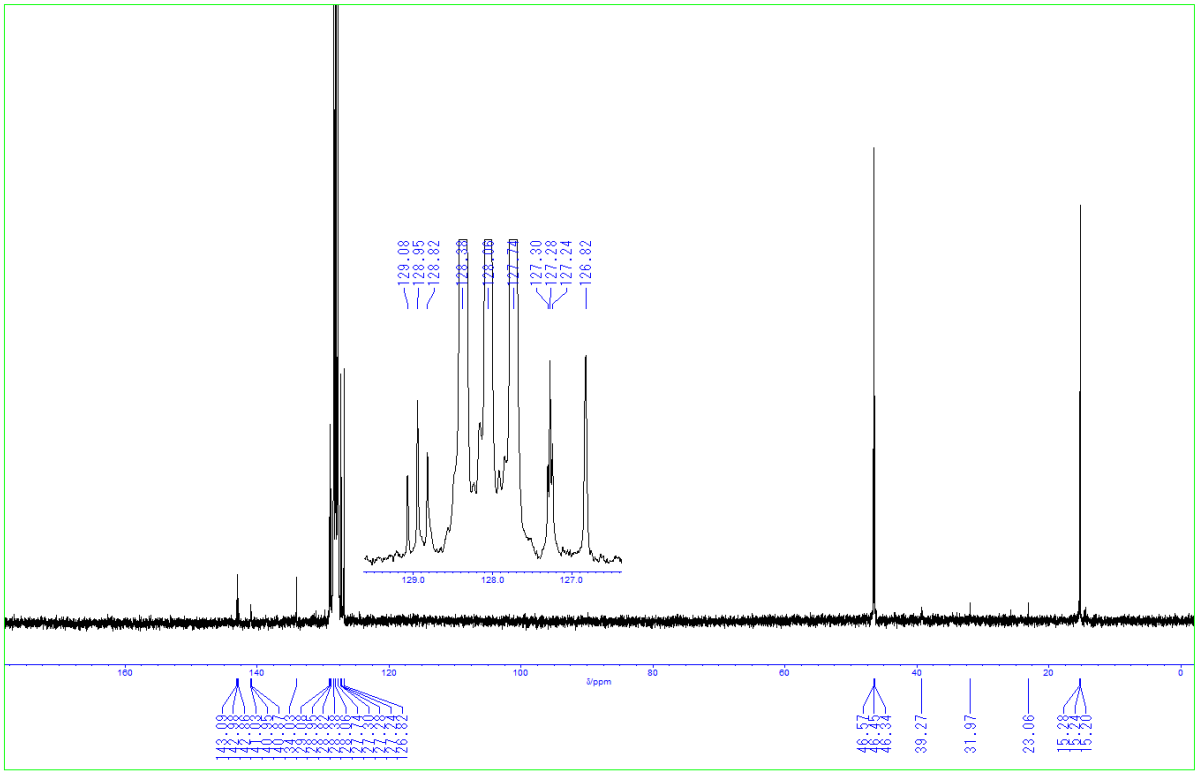

Fig. S11. A $^{13}C\{^{1}H\}$ NMR spectrum of naphthylene-1,8-$Et_2NP–PNEt_2$ **5**

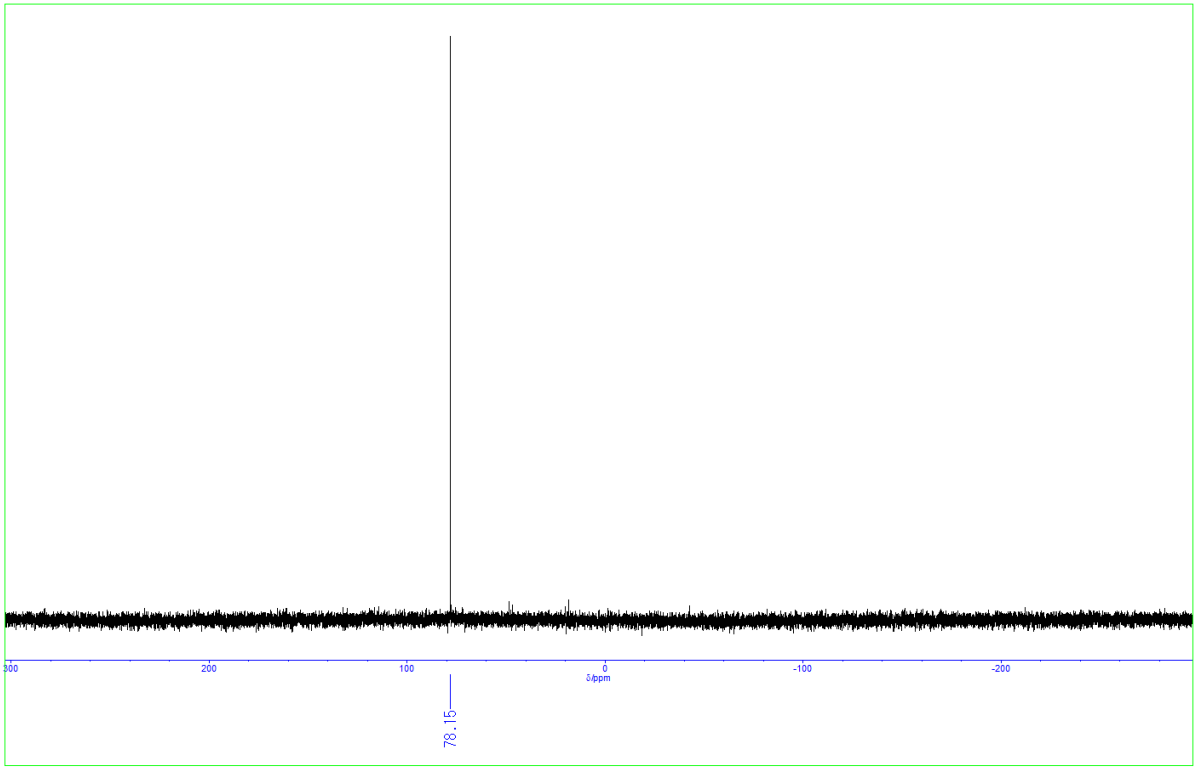

Fig. S12. A $^{31}P\{^{1}H\}$ NMR spectrum of naphthylene-1,8-$Et_2NP–PNEt_2$ **5**

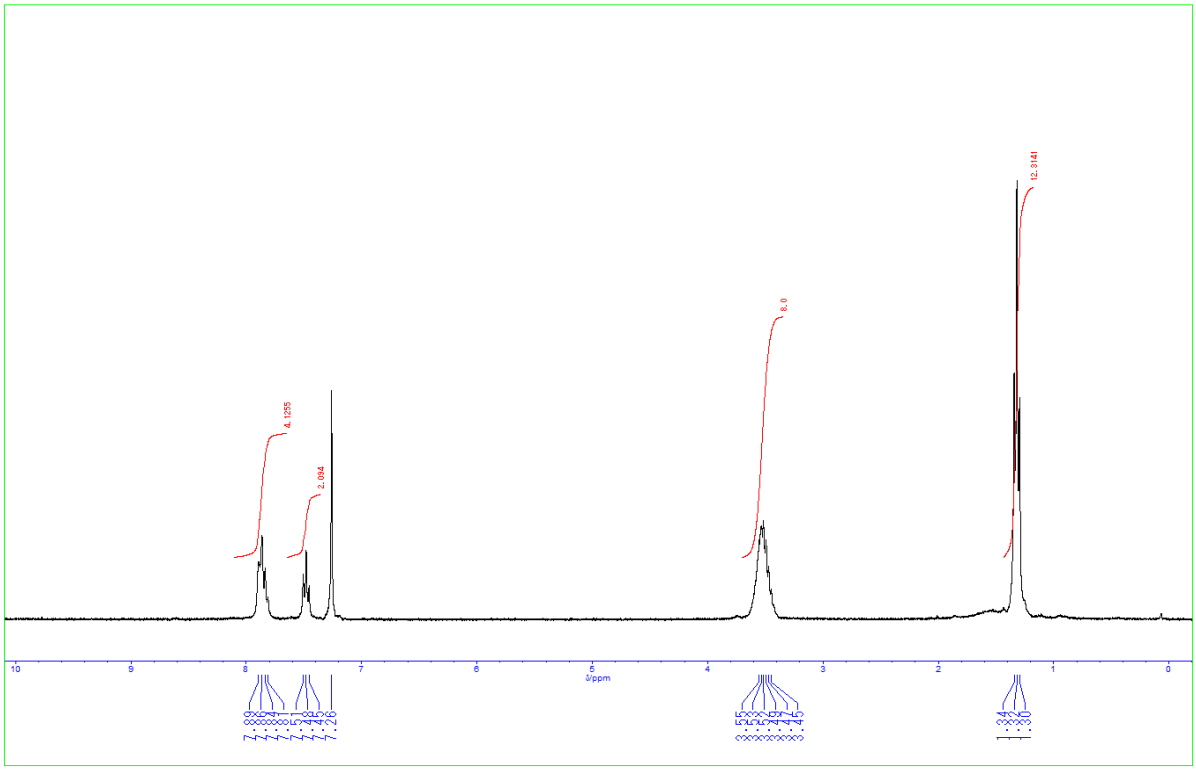

Fig. S13. A ^{1}H NMR spectrum of (μ-5')$[Fe(CO)_3]_2$ **3**

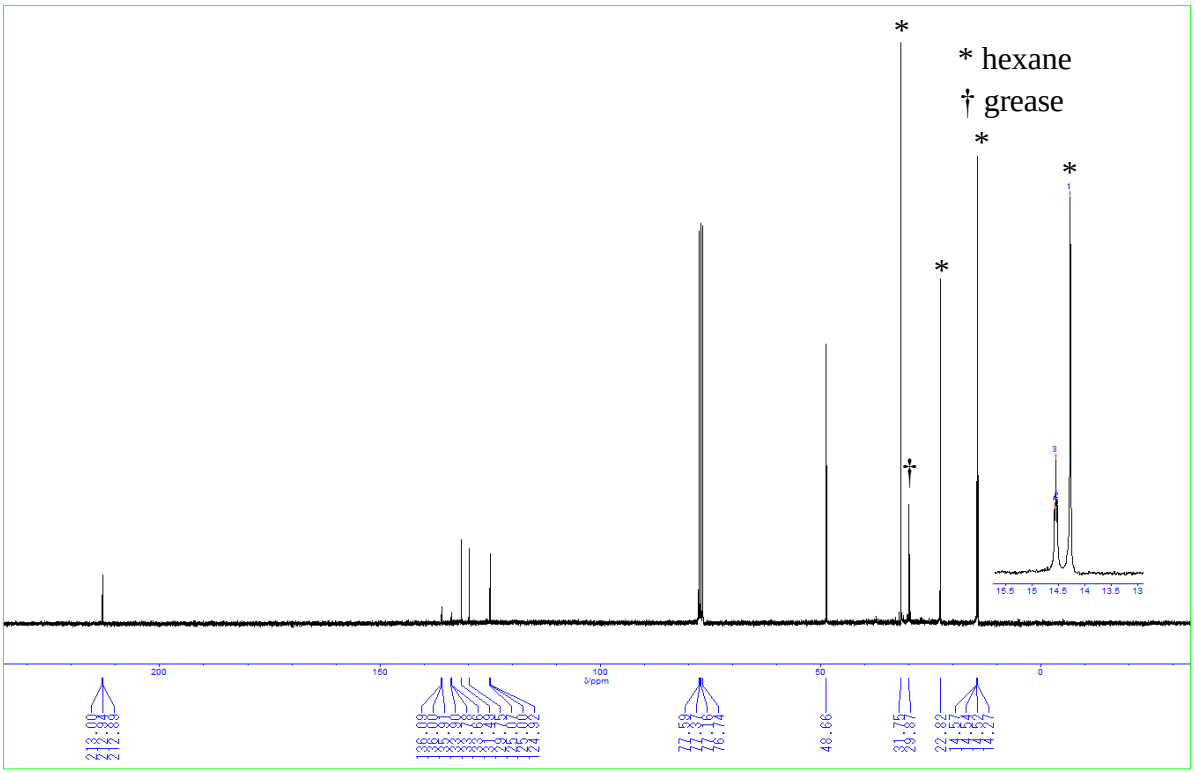

Fig. S14. A $^{13}C\{^{1}H\}$ NMR spectrum of (μ-5')$[Fe(CO)_3]_2$ **3**

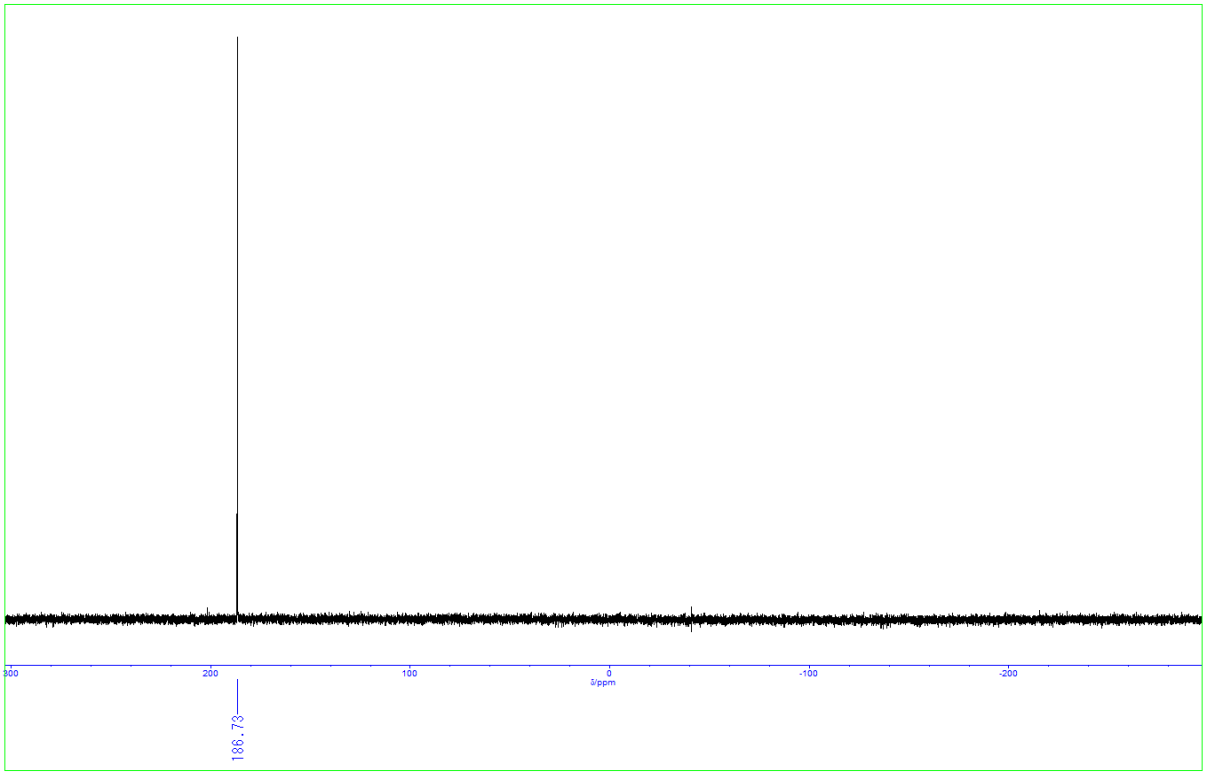

Fig. S15. A $^{31}P\{^{1}H\}$ NMR spectrum of (μ-5')$[Fe(CO)_3]_2$ **3**

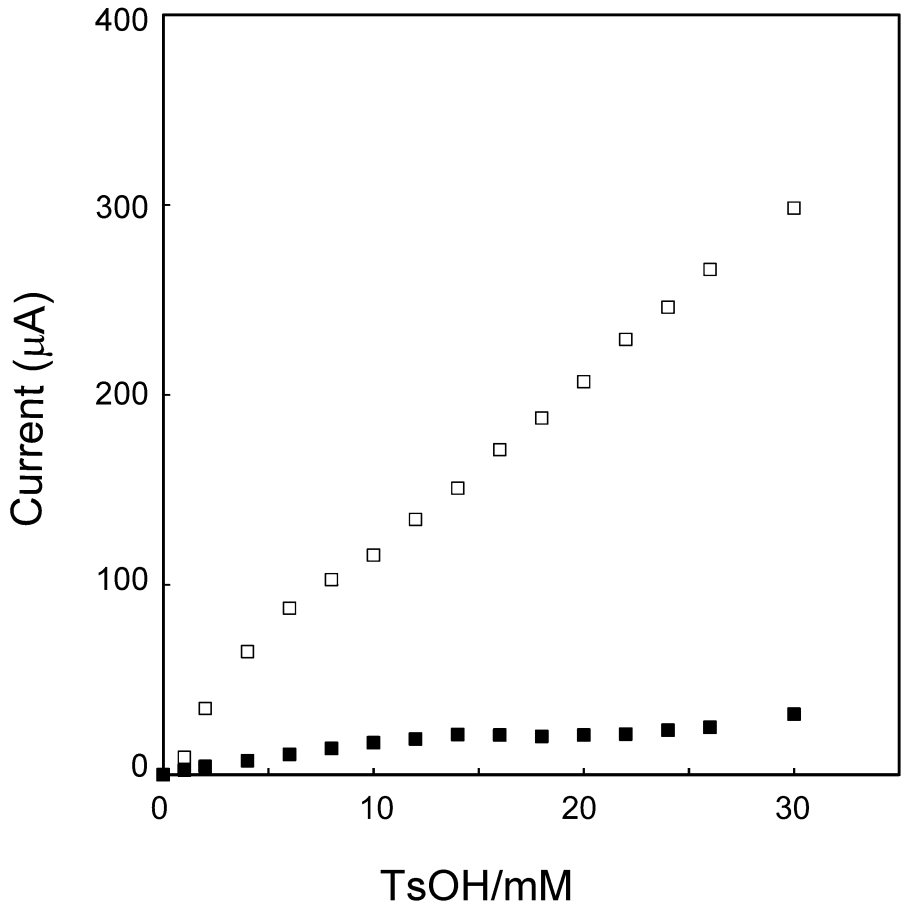

Fig. S16. Plots of TsOH concentration vs increment of the current around -2.2 V (open square) and -1.5 V (closed square).